Photoswitching in diarylethene nanoparticles, a trade-off between bulk solid and solution: towards balanced photochromic and fluorescent properties†

Jonathan Piard,[a] Rémi Métivier,*[a] Marion Giraud,[b] Anne Léaustic,[b] Pei Yu[b] and Keitaro Nakatani*[a]

Received (in Montpellier, France) 30th January 2009, Accepted 25th March 2009
First published as an Advance Article on the web 24th April 2009
DOI: 10.1039/b901800j

Nanoparticles of 1,2-bis[4′-methyl-2′-(2″-pyridyl)thiazolyl]perfluorocyclopentene (**1**) were prepared by laser ablation (355 nm) of microcrystalline powder suspensions in a water–sodium dodecylsulfate medium. AFM studies coupled with microfiltrations reveal that the resulting suspension is mostly made of nanoparticles with 25 ± 10 nm diameters. The resulting yellow transparent colloidal aqueous suspension is both photochromic ($\Phi_{OF\rightarrow CF}$ = 0.20 and $\Phi_{CF\rightarrow OF}$ = 0.96) and fluorescent (Φ_F = 0.017). **1** is not photochromic in the bulk solid, whereas it is only weakly fluorescent in CH_3CN (Φ_F = 0.005); thus, the nanoparticles present a trade-off between these two states where the two properties show reasonable efficiencies. Upon UV irradiation of the opened form of **1**, the fluorescence of the colloidal suspension decreases and shows a bathochromic shift. The emission is recovered upon visible irradiation. Such a behaviour enables us to consider nanoparticles of **1** as a ratiometric fluorescent photoswitch.

Introduction

Among the different properties combined with photochromism in order to obtain photoswitchable systems, fluorescence has been attracting a particularly fast growing interest during the last decade.[1,2] Molecular engineering leads to the design of molecules and materials, which can be more or less classified in three categories: (i) molecules consisting of one single moiety exhibiting both fluorescence and photochromism,[3,4] (ii) multi-component organic molecules and hybrid assemblies (dyads, triads) including metal particles where energy or electron transfer can be reversibly altered by the photochromic moiety,[5–7] and (iii) multi-component polymers where fluorescence is reversibly quenched by a photochromic unit through shielding or energy transfer.[8,9] From such a combination of properties, several applications can be envisaged, from data storage to biological sensing.[6,9–11] One major asset of fluorescence is the possibility of detecting it at the single molecule level, owing to the availability of advanced spectroscopic tools.[12]

Although molecular engineering helps in the design of molecules with some targeted properties, their variation in matrices, assemblies or materials is very difficult to predict.[13] For example, among photochromic molecules, only a few of them keep this property in the bulk state.[1,3,14] However, some advantages can also be drawn from this puzzling influence of the state of the material on physico-chemical properties: quite recently, an enhancement of the fluorescence in nanoparticles of photoswitchable molecules was observed.[15] These objects have drawn the attention of many scientists working on photochromism.[7,11,16,17] In this article, we demonstrate that forming nanomaterials can help to find a balanced trade-off between photochromic and fluorescent properties.

We have previously reported on a diarylethene,[18] 1,2-bis[4′-methyl-2′-(2″-pyridyl)thiazolyl]perfluorocyclopentene (**1**) (Scheme 1). **1** exhibits efficient photochromism, and its opened form (OF) is only weakly fluorescent in acetonitrile solution. Contrarily, the bulk state has completely opposite features: the material is highly fluorescent, but no photochromism was evidenced. This exclusive behaviour was explained as being the result of the competition between fluorescence and photochromism processes, and prevented us from obtaining an efficient fluorescence photoswitching. We report herein on the fabrication of nanoparticles of **1** by laser ablation,[17,19] in order to find a compromise between fluorescence and photochromism in this intermediate state. The nanoparticles were characterized, and their ability to switch the fluorescence in an aqueous colloidal solution was demonstrated.

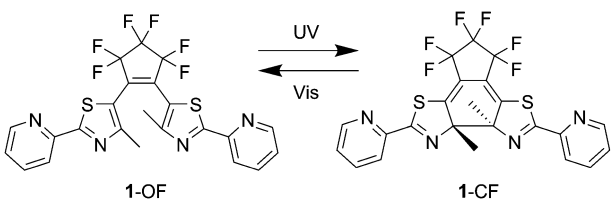

Scheme 1 The photochromic reaction between the opened form (OF) and the closed form (CF) of 1,2-bis[4′-methyl-2′-(2″-pyridyl)thiazolyl]-perfluoro cyclopentene (**1**).

[a] *PPSM, ENS Cachan, CNRS, UniverSud, 61 av President Wilson, 94230 Cachan, France. E-mail: metivier@ppsm.ens-cachan.fr, nakatani@ppsm.ens-cachan.fr*
[b] *LCI, ICMMO, CNRS, University Paris 11, 91405 Orsay, France*
† Electronic supplementary information (ESI) available: AFM images without **1**, absorption and fluorescence spectra of **1** in CH_3CN solution and nanoparticles. See DOI: 10.1039/b901800j

Experimental section

Synthesis and solvents. The organic synthesis of compound **1** has been described previously.[18] A yellow crystalline powder of **1**-OF was obtained. Millipore filtered water (conductivity $< 6 \times 10^{-8}\ \Omega^{-1}\ cm^{-1}$ at 20 °C) was employed as an aqueous solvent for the laser ablation experiments and spectroscopy.

Deposition substrates. Microscope cover slip substrates (Roth) were carefully cleaned in a water–surfactant ultrasonic bath for 30 min, washed in distilled water, sonicated in ethanol for 30 min and dried for 2 h at 80 °C prior to use.

Polycrystalline thin film preparation

Vapor deposition method. The deposition of thin films was carried out using a Leybold vacuum chamber. The crystalline powder (15 mg) from the synthesis was introduced into the crucible (∅ = 10 mm × 25 mm long quartz cylinder) and heated in a furnace by a tungsten filament at a rate of 10 °C min^{-1} (from 25 to 165 °C). The temperature was controlled by a thermocouple. The deposition pressure ($1–2 \times 10^{-5}$ mbar) was fixed by an exhaust vacuum system. Organic molecules were condensed from the vapor phase onto a microscope cover glass substrate positioned behind a mechanically operated shutter. The growth rate was monitored *in situ* by a piezoelectric quartz crystal microbalance. Part of the substrate was hidden to prevent the material deposition, and to allow the measurement of the thickness of the deposited material by atomic force microscope (AFM). The thickness was estimated to be ~400 nm by this method.

Nanoparticles synthesis and characterization

Fabrication of nanoparticles. Nanoparticles were prepared by the laser ablation method following a previously described procedure.[17,19] First, micrometer-sized crystals of **1**-OF (0.3 mg, 5.7×10^{-7} mol) were put into a quartz cuvette (1 cm optical path length), containing an aqueous solution of sodium dodecyl sulfate (SDS, 0.025 M, 3 mL). Then the mixture was simultaneously stirred using a magnetic stirrer and exposed to the third harmonics (355 nm) of a nanosecond Nd:YAG laser (20 mJ $pulse^{-1}$ cm^{-2}, 7 ns full-width at half-maximum pulses, 10 Hz repetition rate) for 16 min at room temperature. The laser ablation process was followed by UV-visible spectrometry. Finally, the suspension was filtered using an MF-Millipore membrane (220 nm pore size) to remove dust traces. Further spectroscopic investigations were performed directly on this aqueous medium.

Size characterization. Droplets of the colloidal suspension were deposited and left on a microscope glass substrate. Topographic images and section profiles of the deposited suspension were performed using an Explorer AFM (Veeco) in ambient atmosphere. The scanner allowed 100 μm displacement in the X–Y directions corresponding to the substrate plane. The images were obtained in tapping mode using a silicon non-contact probe (tip radius <15 nm). The precision of the measurement was ±2 nm in the Z-axis. Several images from 5 μm × 5 μm up to 20 μm × 20 μm dimensions were carried out to evaluate the homogeneity of particles' deposition. Size distributions were obtained from AFM images by Igor-implemented home-made software (Wavemetrics).

Steady-state spectroscopy

UV-visible and fluorescence spectroscopy. Steady-state spectroscopy measurements on colloidal suspensions in water were performed using standard quartz cuvettes. UV-visible spectra were recorded on an Uvikon-940 Kontron spectrometer with an aqueous solution of SDS (0.025 M, 3 mL) as a reference. Corrected emission spectra were recorded on a Jobin-Yvon Spex Fluorolog 1681 fluorometer. The fluorescence quantum yields were determined by using quinine sulfate dihydrate in sulfuric acid (0.5 N) as a standard (Φ_F = 0.546). For the bulk solid state (crystalline powder and thin film), emission spectra and quantum yield measurements of **1**-OF were performed on a C9920-02 Hamamatsu Absolute PL Quantum Yield Measurement System.

Photochromism studies. The photochromic reaction was induced *in situ* by a continuous wavelength irradiation Hg/Xe lamp (Hamamatsu, LC6 Lightingcure, 200 W) equipped with narrow band interference filters of appropriate wavelengths (Semrock Hg01 for λ_{irr} = 365 nm, Oriel 436FS10-25 for λ_{irr} = 436 nm). The irradiation power was measured using a photodiode from Ophir (PD300-UV). The photochromic quantum yields were determined by probing the sample with a xenon lamp during the photochromic reaction. Absorption changes were monitored by a CCD camera mounted with a spectrometer (Princeton Instruments). Kinetic profiles were analysed by Igor-implemented home-made software.

Results and discussion

Fabrication of nanoparticles by the laser ablation method

Nanoparticles of diarylethene **1** were produced as a colloidal suspension through the laser ablation method.[17,19] Organic synthesis yielded **1** in its opened form as microcrystalline powder. A few hundred micrograms were introduced into a quartz cuvette containing an aqueous solution of surfactant (SDS). The concentration of surfactant was chosen three times above the critical micellar concentration (CMC = 8×10^{-3} M for SDS) in order to substantially stabilize the suspension of micro- or nanoparticles. Indeed, too low concentrations of surfactant drove the suspension to a heterogeneous mixture containing crystal sediments, and the laser ablation turned out to be inefficient. The absorption spectrum of the initial suspension of **1**-OF is shown in Fig. 1: a slight scattering and a very weak absorption were observed over the whole UV-visible range (220–600 nm), denoting the small number of large particles present in the suspension before laser ablation. When exposed to the powerful beam of a nanosecond-pulsed laser (20 mJ $pulse^{-1}$ cm^{-2}), the absorbance increased dramatically, as shown in Fig. 1. The experiment was repeated at lower laser fluences and the same spectral evolution was observed; however, the level of absorbance reached after an equivalent energy input was lower. The absorbance increase during the laser ablation is attributed to

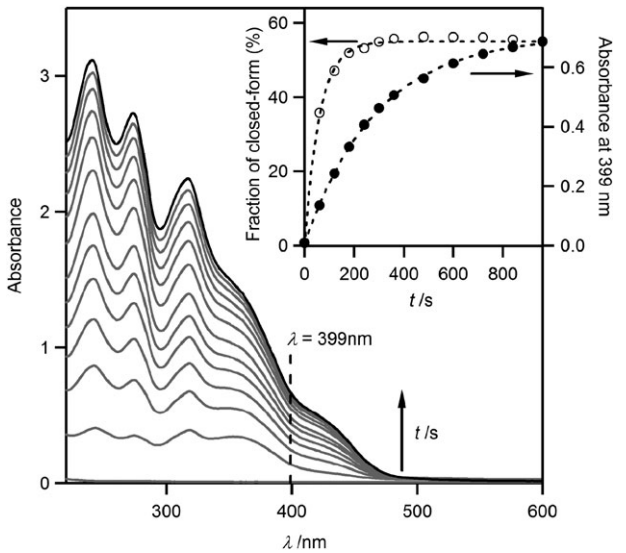

Fig. 1 Evolution as a function of time of the absorption spectra of **1** (0.3 mg in 3 mL of a water–SDS solution at 0.025 M) during the laser-ablation process at 355 nm. Inset: profiles of the absorbance at 399 nm and of the relative concentration of **1**-CF as a function of laser ablation time.

the light-induced fragmentation of the matter. Indeed, during the concomitant increase of the number of particles and the decrease of their average size to the nanometric range, absorption takes over scattering, as already observed.[17] However, the absorption bands do not increase uniformly: simultaneously to the fragmentation, the 355 nm beam is absorbed by **1** and induces the OF → CF reaction. The kinetics of these two phenomena were compared. On the one hand, the absorption time profile at 399 nm, corresponding to the isosbestic point of the **1**-OF–**1**-CF mixture (see next section), was followed in order to appreciate the kinetics of the ablation process. On the other hand, from the data recorded at 399 nm and at 420 nm, the fraction of the closed form, x_{CF}, was determined as follows:

$$x_{CF}(t) = \frac{(A_{420}/A_{399})_t - (A_{420}/A_{399})_{OF}}{(A_{420}/A_{399})_{CF} - (A_{420}/A_{399})_{OF}} \qquad (1)$$

where A_{420} and A_{399} denote the absorbance measured at 420 nm (where **1**-CF absorbs strongly but not **1**-OF) and 399 nm, respectively, and the subscripts OF and CF are related to the absorbance ratios of the pure opened and closed form of **1**, respectively. The comparison of these time profiles indicates that the photochromic reaction already occurs efficiently at the very beginning of the laser shots, leading to a photostationary state within 3 min, whereas the ablation process was still effective even after 16 min. Contrary to the initial time, where the laser ablation occurs mainly on **1**-OF microcrystals, it is evidenced that during most of the ablation time, the materials fragmented into smaller particles is made of a mixture of opened and closed forms. We may conclude that both processes take place at the same time, but the photochromic reaction occurs significantly faster than the laser-induced fragmentation of the matter.

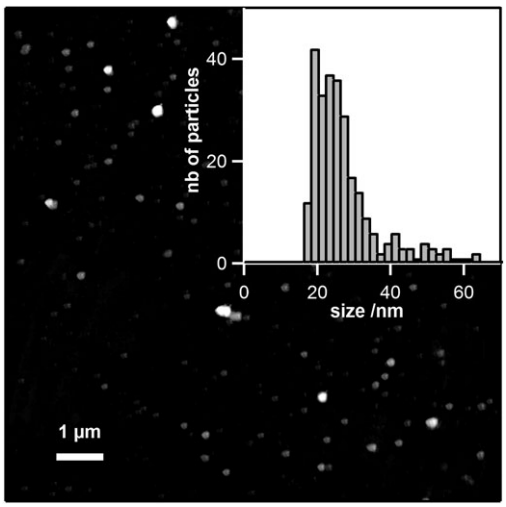

Fig. 2 Atomic force microscopy (AFM) image of nanoparticles of **1** prepared by laser ablation and deposited in a glass substrate. Inset: size distribution of the nanoparticles. The histogram was obtained by the analysis of several AFM images measured at different locations on the sample.

After 16 min of ablation, one drop of the colloidal suspension of **1** was deposited on a glass substrate and AFM images were recorded (Fig. 2). The resulting nanoparticles were clearly identified on the surface, and the size distribution was determined. The vast majority of the particles were found to have a 25 ± 10 nm diameter. In the present case, the laser ablation method produced a well-defined monodisperse colloidal suspension of organic particles. The suspension was stable, without noticeable aggregation for a few days. We confirmed the small amount of large particles by successive microfiltration experiments (MF-Millipore membranes from 800 nm down to 50 nm pore size) combined with absorption spectra showing that particles larger than 50 nm contributed to only 10% of the overall absorption spectrum. Although we cannot exclude a partial dissolution of **1** in SDS, comparison of AFM images and spectra gives some evidence of the formation of nanoparticles of **1** (see the ESI†).

Photochromic properties of nanoparticles compared to the solution and the solid state

As shown in the previous paragraph (Fig. 1, inset), the laser ablation procedure at 355 nm produced a colloidal suspension of nanoparticles, with an OF–CF composition corresponding to the photostationary state at 355 nm (Fig. 3, curve B). The absorption spectrum of **1**-OF was then obtained after irradiation by visible light at 436 nm (Fig. 3, curve A), where only **1**-CF absorbs. The band maxima are very similar to those in CH_3CN: λ_{max} = 354 nm in **1**-OF nanoparticles while λ_{max} = 358 nm in a solution of **1**-OF (see full spectra in the ESI†).[18] Subsequently, under irradiation at 365 nm, the colloidal suspension reached a new photostationary state, as displayed in Fig. 3, curve C. All three absorption spectra (Fig. 3, curves A to C) show a clear isosbestic point at 399 nm. In the present case, the closed form absorbs light over the whole UV range, so we could not experimentally obtain a 100% pure sample of the closed form. Therefore,

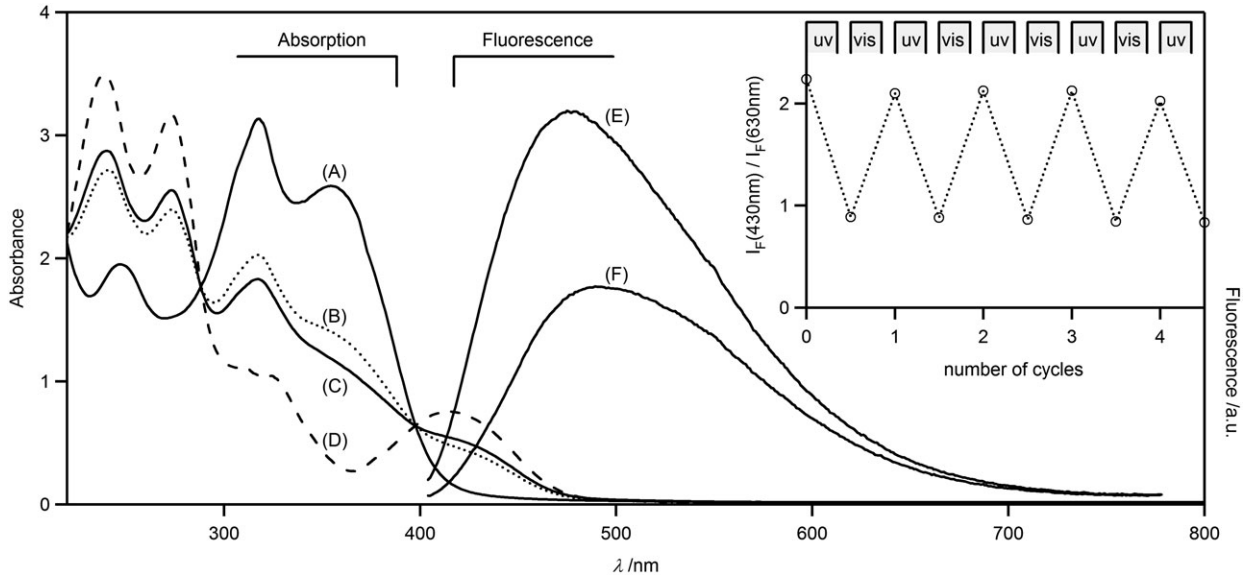

Fig. 3 UV-Vis absorption spectra and fluorescence spectra of nanoparticles of **1** in different states: (A) absorption spectrum of **1**-OF, (B) and (C) absorption spectrum of **1** at the photostationary state at 355 nm and 365 nm, respectively, (D) extrapolated absorption spectrum of **1**-CF determined by Fischer's method, (E) fluorescence spectrum of **1**-OF, and (F) fluorescence spectrum of **1** at the photostationary state at 365 nm. Inset: photoswitching of the ratio of the fluorescence intensities at 430 nm and 630 nm under alternating irradiation at 365 nm (UV, 135 mW for 30 sec) and 436 nm (visible, 10 mW for 30 sec). All fluorescence spectra were excited at the isosbestic point (λ_{exc} = 399 nm).

Fischer's method was applied to our system in order to obtain the absorption spectrum of pure **1**-CF (see Appendix).[20] It allowed us to determine the conversion yields of the two photostationary states: α(355 nm) = 0.53 and α(365 nm) = 0.63. From these values, we could extrapolate the **1**-CF absorption spectrum depicted in Fig. 3, curve D. As already mentioned for the opened form, the band maxima of **1**-CF appear to be comparable to the solution (λ_{max} = 414 nm in both cases). The molar absorption coefficients were assumed to have the same values in CH_3CN and in nanoparticles at the isosbestic point: ε(399 nm) = 4500 M^{-1} cm^{-1}. The value for nanoparticles at any other wavelength, λ, was deduced from:

$$\varepsilon_i(\lambda) = \varepsilon(399\ \text{nm}) \times (A_\lambda)_i/(A_{399})_i \qquad (2)$$

where i = OF or CF, and $(A_\lambda)_i$ and $(A_{399})_i$ denote the absorbance of the nanoparticles of the pure i species at wavelengths λ and 399 nm, respectively.

The quantum yields of the cyclization ($\Phi_{OF\rightarrow CF}$) and ring-opening reactions ($\Phi_{CF\rightarrow OF}$) at room temperature were measured by irradiating the samples with an Hg/Xe lamp through appropriate band-pass filters (see experimental section for details). The photochromic quantum yields of **1** were previously measured in a CH_3CN solution (Table 1) and no thermal back reaction was observed.[18] We could not induce the photochromic reaction in the bulk state, even at high irradiation power, for both crystalline powder and polycrystalline thin films. Interestingly, the colloidal suspension of nanoparticles showed intermediate photochromic properties halfway between the solution and solid state. As reported in Table 1, the cyclization quantum yield of nanoparticles (0.20) is lower than in CH_3CN solution (0.50). Conversely, the backward quantum yield was measured to be higher in colloidal suspension (0.96) than in solution (0.52). Thus, the following tendencies can be established: from the solution to the nanoparticles and the bulk states, $\Phi_{OF\rightarrow CF}$ continuously decreases down to zero. $\Phi_{CF\rightarrow OF}$ is higher in nanoparticles than in solution and its value in bulk solid could not be determined, since the initial opened form could not be converted to the closed form. These trends lead us to conclude that in case of compound **1**, when the molecules are not constrained, as in solution, photochromism can fully arise. But when the environment becomes more rigid, such as in the crystal state, conformational changes may be hindered, the ratio $\Phi_{OF\rightarrow CF}$: $\Phi_{CF\rightarrow OF}$ decreases, and the equilibrium of the photostationary state is displaced to the opened form. According to these schematic considerations, the nanoparticles show interesting behaviour as an intermediate state between the solution and solid state. Because of their small sizes and large surface-to-volume ratio, the molecular

Table 1 Photochromic and fluorescence quantum yields of **1** in solution, nanoparticles, and bulk states

	Photochromism[a]		Fluorescence[b]	
	$\Phi_{OF\rightarrow CF}$	$\Phi_{CF\rightarrow OF}$	Φ_{OF}	Φ_{CF}
CH_3CN solution	0.50[c]	0.52[c]	0.005[c]	$<10^{-4}$
Nanoparticles[d]	0.20	0.96	0.017	>0.008[e]
Bulk solid[f]	0	—[g]	0.2	—[g]

[a] Photochromic quantum yields are given ±10%. λ_{irr}(OF → CF) = 365 nm and λ_{irr}(CF → OF) = 436 nm. [b] Fluorescence quantum yields are given ±10%. [c] From ref. 18. [d] Colloidal suspension in water. [e] This lower limit value was extrapolated from the photostationary state neglecting the contributions of radiative and non-radiative energy transfer. [f] The quantum yield values are similar for crystalline powder and vapor-deposited polycrystalline thin film. [g] The absence of the photochromic reaction OF → CF prevented such measurements.

arrangement and the crystal lattice of nanoparticles may actually be less rigid than in the bulk crystal.

Fluorescence and photoswitching properties of colloidal suspension of nanoparticles

According to our previous work in CH_3CN solution,[18] the fluorescence quantum yield is very weak for the opened form ($\Phi_F = 0.005$) and below the detection limit for the closed form (Table 1). Photoswitching was demonstrated, but the low signal-to-noise ratio precludes any reasonable application of this feature. On the other side, despite its lack of photochromism, the solid state is strongly emitting and the fluorescence quantum yield, measured by means of an integration sphere (see experimental section for details), reaches 0.2. Nanoparticles displayed attractive fluorescence features compared to the solution and the bulk state. Indeed, the fluorescence spectrum of **1**-OF has a maximum located at 475 nm (Fig. 3, curve E), and the fluorescence quantum yield was determined for the colloidal suspension to be 0.017, which is more than three times as high as in CH_3CN solution. We would like to stress that the fluorescence emission is usually lower in aqueous media compared to organic solvents, so that such an improvement from CH_3CN solution is quite appreciable.[21] Under irradiation at 365 nm, the photostationary state was reached and the fluorescence was reduced down to 60% of the **1**-OF form. Contrary to the behaviour in solution, the fluorescence of the photostationary state in nanoparticles was still intense and the emission maximum was red-shifted to 490 nm (Fig. 3, curve F). These valuable properties allow a ratiometric measurement of the photoswitching properties. The emission ratio I_F(430 nm) : I_F(630 nm) as the response of the photoswitching system has a considerable interest, since the ratio of these fluorescence intensities is independent of the total concentration of nanoparticles, and avoids problems related to the fluctuations of the source intensity and to the sensitivity of the instrument.[21] Several switching cycles of this emission ratio were recorded under alternating UV and visible irradiation without degradation of the properties. At this stage of our study, one should emphasize that the switching behaviour of fluorescent photochromic systems comes from a subtle combination of two properties: the photochromic reaction, that induces the change of the state of the photoactive site (“writing” step), and the fluorescence process, that is responsible for the detection of the state of the system (“reading” step). The molecular system, **1**, is a typical example of the competition between both properties, which are held by a unique molecular entity. In CH_3CN solution, **1** displays too weak fluorescence, while it shows no photochromism in the solid state. Definitively, nanoparticles of **1** represent an appropriate compromise between the solution and the bulk state, and exhibit attractive photoswitching properties which can be exploited in the ratiometric mode.

The red-shift and diminishing of the nanoparticles fluorescence at the photostationary state may be tentatively explained by three different factors, arising when the CF molecules are generated: (i) radiative energy transfer, (ii) non-radiative energy transfer, and (iii) lower emitting properties of **1**-CF itself compared to **1**-OF. Concerning the first factor, the overlap between the emission band of **1**-OF and the absorption band of **1**-CF can lead to an emission–reabsorption process. However, we evaluated the contribution of this effect to be less than 5% of the fluorescence decrease in the present case. Moreover, the excitation inner filter effect has no influence, since fluorescence was recorded by excitation at the isosbestic point. Regarding the second factor, the spectral overlap between the fluorescence spectrum of **1**-OF and the absorption spectrum of **1**-CF is appreciable (Fig. 3). Assuming as a first approximation that such an energy transfer would be predominantly governed by dipole–dipole interactions, we used Förster’s theory to evaluate the extent of such a process.[22] The Förster critical radius, R_0, is given by the following equation:

$$R_0 = 0.2108[\kappa^2 \Phi_{OF} n^{-4} \int_0^\infty F_{OF}(\lambda)\varepsilon_{CF}(\lambda)\lambda^4 d\lambda]^{1/6} \qquad (3)$$

with R_0 in Å, where κ^2 is the orientational factor, n the average refractive index of the medium in the wavelength range where spectral overlap is significant, $F_{OF}(\lambda)$ is the normalized fluorescence spectrum of the opened form, and λ the wavelength in nanometres. The refractive index was chosen to be 1.55, a value reported for a comparable diarylethene.[23] Owing to the crystal structure of **1**, different transition moment dipole orientations are possible in the crystal frame. Thus, depending on the orientation factor (from 0.7 to 4), the Förster radius was found to be between 13 and 18 Å. These values mean that non-radiative energy transfer probably takes place within the nanoparticles. More detailed steady-state and time-resolved fluorescence studies are necessary to estimate this contribution with a better accuracy. The third factor concerns the fluorescence properties of the closed form itself. We estimated the contribution of the closed form to the emission spectrum of the photostationary state. This was possible, since the composition of the photostationary state and the emission spectrum of **1**-OF are known. A quantum yield of 0.008 for **1**-CF was obtained, assuming that the fluorescence of the two forms, OF and CF, were additive. In other words, factors (i) and (ii) (radiative and non-radiative energy transfers) were neglected in this determination, and this value has to be considered as a lower limit.

Conclusions

The contrast of fluorescence between the emitting and the non-emitting states is usually considered as a figure of merit in fluorescent photochromes. Here, we presented a complementary approach, based on the ratio of fluorescence emitted at two different wavelengths. The evolution of this ratio can be followed in photochromic systems where both photoisomers emit in different wavelength ranges. Such a ratiometric method has an important asset, for example in sensing, since the measured ratio is independent of the concentration of chromophores.

Laser ablation is a reliable method to obtain nanoparticles. Although relatively expensive in energy, it avoids the use of organic solvents, and allows one to obtain aqueous colloidal suspensions of insoluble molecules with good optical properties (no scattering, for instance). Nanoparticles obtained by this sophisticated technique allowed us to reach a

trade-off between fluorescence and photochromism, which are competitively coexisting in **1**. Contrary to other states (such as bulk solid), exclusiveness of either property was avoided, and both properties showed reasonable efficiencies, which is essential for applications involving photochromism as writing and fluorescence as reading functions.

Appendix

The absorption spectrum of the closed form was determined by the Fischer's method.[20] It is applicable for systems without thermal relaxation. Under this condition, the photostationary states are extrapolated to infinite irradiation time. The ratio of the equilibrium concentrations of the opened (C_{OF}) and closed forms (C_{CF}) at a given photostationary state is expressed as follows:

$$\frac{C_{OF}}{C_{CF}} = \frac{\Phi_{CF\rightarrow OF} \times \varepsilon_{CF}}{\Phi_{OF\rightarrow CF} \times \varepsilon_{OF}} = \frac{\Phi_{CF\rightarrow OF} \times A_{CF}}{\Phi_{OF\rightarrow CF} \times A_{OF}} \qquad \text{(A1)}$$

where ε_{OF} and ε_{CF} are the molar absorption coefficients of the opened and closed forms, and A_{OF} and A_{CF} stand for the absorption of a sample of same chromophore concentration containing only the opened or closed form, respectively. By comparing the photostationary states obtained under irradiation at two different wavelengths λ' and λ'', a couple of equations of type (A1) are obtained. Assuming that the ratio $\Phi_{CF\rightarrow OF} : \Phi_{OF\rightarrow CF}$ does not depend on the irradiation wavelength, we get:

$$\left(\frac{C'_{OF}}{C'_{CF}}\right) \Big/ \left(\frac{C''_{OF}}{C''_{CF}}\right) = \left(\frac{A'_{CF}}{A'_{OF}}\right) \Big/ \left(\frac{A''_{CF}}{A''_{OF}}\right) \qquad \text{(A2)}$$

If we introduce the OF → CF conversion yield, α, eqn (A2) evolves to:

$$\left(\frac{1-\alpha'}{\alpha'}\right) \Big/ \left(\frac{1-\alpha''}{\alpha''}\right) = \left(\frac{A'_{CF}}{A'_{OF}}\right) \Big/ \left(\frac{A''_{CF}}{A''_{OF}}\right) \qquad \text{(A3)}$$

In order to introduce experimental data into eqn (A3), we can write that the absorbance, A, measured at any particular wavelength, λ, of a mixture of opened and closed forms, where the overall concentration $C_{OF} + C_{CF}$ is constant, is given by:

$$A = (1-\alpha)A_{OF} + \alpha A_{CF}$$
$$\text{or } A_{CF} = A_{OF} + \frac{(A - A_{OF})}{\alpha} \qquad \text{(A4)}$$

This can be combined with eqn (A3) to yield:

$$\left(\frac{1-\alpha'}{\alpha'}\right) \Big/ \left(\frac{1-\alpha''}{\alpha''}\right) = \left(1+\frac{\Delta'}{\alpha'}\right) \Big/ \left(1+\frac{\Delta''}{\alpha''}\right) \qquad \text{(A5)}$$

where $\Delta = (A - A_{OF})/A_{OF}$ and denotes the relative change of absorbance observed when a solution of opened form is irradiated to the photostationary state. Furthermore, the ratio $\rho = \alpha'/\alpha''$ of the conversion yields at two different photostationary states, resulting from irradiation at two different wavelengths, is equal to the ratio of the Δ's measured at any given wavelength (the wavelength that maximizes the Δ's is usually chosen). Equating and developing (A5) yields the final formula:

$$\alpha'' = \frac{\Delta' - \Delta''}{1 + \Delta' - \rho(1 + \Delta'')} \qquad \text{(A6)}$$

where all the parameters Δ and ρ are experimentally accessible. The numerical value of α'' determined by this equation may then be used to calculate the absorption spectrum of the pure closed form by means of eqn (A4).

Acknowledgements

We are grateful to A. Brosseau for his assistance in AFM and vapor deposition experiments. Solid state fluorescence measurements by courtesy of Hamamatsu Photonics France. The PNANO program from the Agence Nationale de la Recherche (ANR, France) is acknowledged for its financial support.

References

1 M. Irie, *Chem. Rev.*, 2000, **100**, 1685–1716.
2 B. L. Feringa, *Molecular Switches*, Wiley-VCH, Darmstadt, 2001; K. Matsuda and M. Irie, *J. Photochem. Photobiol., C*, 2004, **5**, 169–182; H. Tian and S. J. Yang, *Chem. Soc. Rev.*, 2004, **33**, 85–97; F. M. Raymo and M. Tomasulo, *Chem. Soc. Rev.*, 2005, **34**, 327–336; F. M. Raymo and M. Tomasulo, *J. Phys. Chem. A*, 2005, **109**, 7343–7352; D. Gust, T. A. Moore and A. L. Moore, *Chem. Commun.*, 2006, 1169–1178; H. Tian and S. Wang, *Chem. Commun.*, 2007, 781–792; *Organic Photochromic and Thermochromic Compounds*, ed. J. C. Crano and R. J. Guglielmetti, Plenum, New York, 1999.
3 T. Fukaminato, T. Kawai, S. Kobatake and M. Irie, *J. Phys. Chem. B*, 2003, **107**, 8372–8377; Y. C. Jeong, S. I. Yang, K. H. Ahn and E. Kim, *Chem. Commun.*, 2005, 2503–2505.
4 M. Giraud, A. Leaustic, R. Guillot, P. Yu, P. G. Lacroix, K. Nakatani, R. Pansu and F. Maurel, *J. Mater. Chem.*, 2007, **17**, 4414–4425; F. Li, J. P. Zhuang, G. Y. Jiang, H. H. Tang, A. D. Xia, L. Jiang, Y. L. Song, Y. L. Li and D. B. Zhu, *Chem. Mater.*, 2008, **20**, 1194–1196; M. A. L. Sheepwash, R. H. Mitchell and C. Bohne, *J. Am. Chem. Soc.*, 2002, **124**, 4693–4700.
5 M. Berberich, A. M. Krause, M. Orlandi, F. Scandola and F. Wurthner, *Angew. Chem., Int. Ed.*, 2008, **47**, 6616–6619; B. Z. Chen, M. Z. Wang, Y. Q. Wu and H. Tian, *Chem. Commun.*, 2002, 1060–1061; I. L. Medintz, S. A. Trammell, H. Mattoussi and J. M. Mauro, *J. Am. Chem. Soc.*, 2004, **126**, 30–31; G. Y. Jiang, S. Wang, W. F. Yuan, L. Jiang, Y. L. Song, H. Tian and D. B. Zhu, *Chem. Mater.*, 2006, **18**, 235–237; J. Andreasson, S. D. Straight, S. Bandyopadhyay, R. H. Mitchell, T. A. Moore, A. L. Moore and D. Gust, *J. Phys. Chem. C*, 2007, **111**, 14274–14278; S. Z. Wu, Y. L. Luo, F. Zeng, J. Chen, Y. N. Chen and Z. Tong, *Angew. Chem., Int. Ed.*, 2007, **46**, 7015–7018; R. H. Mitchell, C. Bohne, S. G. Robinson and Y. H. Yang, *J. Org. Chem.*, 2007, **72**, 7939–7946; H. Yamaguchi, K. Matsuda and M. Irie, *J. Phys. Chem. C*, 2007, **111**, 3853–3862; L. Y. Zhu, W. W. Wu, M. Q. Zhu, J. J. Han, J. K. Hurst and A. D. Q. Li, *J. Am. Chem. Soc.*, 2007, **129**, 3524–3526; M. Tomasulo, E. Deniz, R. J. Alvarado and F. M. Raymo, *J. Phys. Chem. C*, 2008, **112**, 8038–8045; H. Zhao, U. Al-Atar, T. C. S. Pace, C. Bohne and N. R. Branda, *J. Photochem. Photobiol., A*, 2008, **200**, 74–82.
6 V. Ferri, M. Scoponi, C. A. Bignozzi, D. S. Tyson, F. N. Castellano, H. Doyle and G. Redmond, *Nano Lett.*, 2004, **4**, 835–839.
7 J. Folling, S. Polyakova, V. Belov, A. van Blaaderen, M. L. Bossi and S. W. Hell, *Small*, 2008, **4**, 134–142.
8 Y. Chen and N. Xie, *J. Mater. Chem.*, 2005, **15**, 3229–3232; Y. F. Feng, Y. L. Yan, S. Wang, W. H. Zhu, S. X. Qian and

H. Tian, *J. Mater. Chem.*, 2006, **16**, 3685–3692; S. M. Lewis and E. J. Harbron, *J. Phys. Chem. C*, 2007, **111**, 4425–4430; S. Murase, M. Teramoto, H. Furukawa, Y. Miyashita and K. Horie, *Macromolecules*, 2003, **36**, 964–966.

9 C. C. Corredor, Z. L. Huang and K. D. Belfield, *Adv. Mater.*, 2006, **18**, 2910–2914; C. C. Corredor, Z. L. Huang, K. D. Belfield, A. R. Morales and M. V. Bondar, *Chem. Mater.*, 2007, **19**, 5165–5173; R. Métivier, S. Badré, R. Méallet-Renault, P. Yu, R. B. Pansu and K. Nakatani, *J. Phys. Chem. C*, 2009, in press.

10 T. Sakata, D. K. Jackson, S. Mao and G. Marriott, *J. Org. Chem.*, 2008, **73**, 227–233.

11 M.-Q. Zhu, L. Zhu, J. J. Han, W. Wu, J. K. Hurst and A. D. Q. Li, *J. Am. Chem. Soc.*, 2006, **128**, 4303–4309; L. Y. Zhu, M. Q. Zhu, J. K. Hurst and A. D. Q. Li, *J. Am. Chem. Soc.*, 2005, **127**, 8968–8970; S. Wang, W. Shen, Y. L. Feng and H. Tian, *Chem. Commun.*, 2006, 1497–1499; H. G. Zhu and M. J. McShane, *J. Am. Chem. Soc.*, 2005, **127**, 13448–13449.

12 M. Irie, T. Fukaminato, T. Sasaki, N. Tamai and T. Kawai, *Nature*, 2002, **420**, 759–760; T. Fukaminato, T. Sasaki, T. Kawai, N. Tamai and M. Irie, *J. Am. Chem. Soc.*, 2004, **126**, 14843–14849; T. Fukaminato, T. Umemoto, Y. Iwata, S. Yokojima, M. Yoneyama, S. Nakamura and M. Irie, *J. Am. Chem. Soc.*, 2007, **129**, 5932–5938.

13 D. Y. Curtin and I. C. Paul, *Chem. Rev.*, 1981, **81**, 525–541; A. Gavezzotti, *Curr. Opin. Solid State Mater. Sci.*, 1996, **1**, 501–505; J. Hulliger, H. Bebie, S. Kluge and A. Quintel, *Chem. Mater.*, 2002, **14**, 1523–1529; G. R. Desiraju, *J. Mol. Struct.*, 2003, **656**, 5–15.

14 J. N. Moorthy, P. Mal, R. Natarajan and P. Venugopalan, *Org. Lett.*, 2001, **3**, 1579–1582; K. Amimoto and T. Kawato, *J. Photochem. Photobiol., C*, 2005, **6**, 207–226; M. Morimoto and M. Irie, *Chem. Commun.*, 2005, 3895–3905; S. Kobatake, K. Uchida, E. Tsuchida and M. Irie, *Chem. Commun.*, 2002, 2804–2805; S. Z. Pu, J. K. Xu, L. Shen, Q. Xiao, T. S. Yang and G. Liu, *Tetrahedron Lett.*, 2005, **46**, 871–875; J. X. Guo, L. Liu, G. F. Liu, D. Z. Jia and X. L. Xie, *Org. Lett.*, 2007, **9**, 3989–3992; P. Naumov, P. Yu and K. Sakurai, *J. Phys. Chem. A*, 2008, **112**, 5810–5814; P. Naumov, *J. Mol. Struct.*, 2006, **783**, 1–8; M. Kawano, T. Sano, J. Abe and Y. Ohashi, *J. Am. Chem. Soc.*, 1999, **121**, 8106–8107.

15 S. J. Lim, B. K. An, S. D. Jung, M. A. Chung and S. Y. Park, *Angew. Chem., Int. Ed.*, 2004, **43**, 6346–6350; S. J. Lim, J. Seo and S. Y. Park, *J. Am. Chem. Soc.*, 2006, **128**, 14542–14547; T. Fukaminato and M. Irie, *Adv. Mater.*, 2006, **18**, 3225–3228; S. J. Lim, B. K. An and S. Y. Park, *Macromolecules*, 2005, **38**, 6236–6239.

16 F. Sun, F. S. Zhang, F. Q. Zhao, X. H. Zhou and S. Z. Pu, *Chem. Phys. Lett.*, 2003, **380**, 206–212; X. H. Sheng, A. D. Peng, H. B. Fu, Y. Y. Liu, Y. S. Zhao, Y. Ma and J. N. Yao, *Nanotechnology*, 2007, 18; Z. Hu, Q. Zhang, M. Xue, Q. Sheng and Y. G. Liu, *J. Phys. Chem. Solids*, 2008, **69**, 206–210; W. R. Browne, T. Kudernac, N. Katsonis, J. Areephong, J. Hielm and B. L. Feringa, *J. Phys. Chem. C*, 2008, **112**, 1183–1190; S. Spagnoli, D. Block, E. Botzung-Appert, I. Colombier, P. L. Baldeck, A. Ibanez and A. Corval, *J. Phys. Chem. B*, 2005, **109**, 8587–8591.

17 A. Spangenberg, R. Métivier, J. Gonzalez, K. Nakatani, P. Yu, M. Giraud, A. Léaustic, R. Guillot, T. Uwada and T. Asahi, *Adv. Mater.*, 2009, **21**, 309–313.

18 M. Giraud, A. Leaustic, M. F. Charlot, P. Yu, M. Cesario, C. Philouze, R. Pansu, K. Nakatani and E. Ishow, *New J. Chem.*, 2005, **29**, 439–446.

19 H. G. Jeon, T. Sugiyama, H. Masuhara and T. Asahi, *J. Phys. Chem. C*, 2007, **111**, 14658–14663; T. Asahi, T. Sugiyama and H. Masuhara, *Acc. Chem. Res.*, 2008, **41**, 1790–1798; H. Masuhara, T. Asahi and Y. Hosokawa, *Pure Appl. Chem.*, 2006, **78**, 2205–2226.

20 E. Fischer, *J. Phys. Chem.*, 1967, **71**, 3704–3706.

21 B. Valeur, *Molecular Fluorescence: Principles and Applications*, Wiley-VCH, Weinheim, 2002.

22 T. Förster, *Naturwissenschaften*, 1946, **33**, 166; T. Förster, *Ann. Phys.*, 1948, **2**, 55.

23 T. Kawai, N. Fukuda, D. Groschl, S. Kobatake and M. Irie, *Jpn. J. Appl. Phys., Part 2*, 1999, **38**, L1194–L1196.

